± 0.005[1] the present determination of $\alpha = 0.3 \pm 0.1$ leads, with the Griffiths-Rushbrook inequalities (written as equalities),[11] to the values $\gamma = 1.03 \pm 0.11$ and $\delta = 4.07 \pm 0.37$, respectively. Egelstaff and Ring[11] deduce a value of $\delta \approx 4$ from the data of Predel[7] on this system. From the present data it follows that metallic binary mixtures do not show considerably different behavior in the critical region from the nonconducting binaries, and the earlier contention of Egelstaff and Ring[11] that the interatomic forces affect the values of the critical exponents does not seem to hold in this instance.

*Supported by the Office of Naval Research, under Contract No. N00014-67-A-0398-0010.

†Present address: Physics Department, Temple University, Philadelphia, Pa. 19122.

[1]H. K. Schürmann and R. D. Parks, Phys. Rev. Letters 26, 357 (1971).

[2]See also P. D. Adams, Phys. Rev. Letters 25, 1012 (1970); H. K. Schürmann and R. D. Parks, *ibid.* 26, 835 (1971).

[3]M. E. Fisher and J. S. Langer, Phys. Rev. Letters 20, 665 (1968).

[4]F. C. Zumsteg and R. D. Parks, Phys. Rev. Letters 24, 520 (1970).

[5]K. N. Lee, R. Bachmann, T. H. Geballe, and T. P. Maita, Phys. Rev. B 2, 4580 (1970).

[6]D. S. Simons and M. B. Salamon, Phys. Rev. Letters 26, 750 (1971).

[7]The method of differential thermal analysis, which consists of locating singularities in the cooling rate (hence, specific-heat anomalies), has been used in various instances to determine the coexistence curve in binary liquid metals. However, in these studies the specific-heat anomalies were not studied in any detail. For the Ga-Hg system, see B. Predel, Z. Physik. Chem. (Frankfort) 24, 206 (1960).

[8]H. K. Schürmann and R. D. Parks, Phys. Rev. Letters 27, 1790 (1971). In the first paragraph on p. 1793 containing the results in the Ga-Bi system it should read: "Below T_c the two layers formed exhibit resistive behavior which is qualitatively the same as that observed (by us) in the Ga-Hg system [Phys. Rev. Letters 26, 357 (1971); 26, 835 (1971)]. Above T_c the behavior of the uniform mixture was analogous to that observed in the Li-Na system, e.g., $d\rho/dT$ increases as $T \to T_c$ from above, in contradistinction to Adams's results."

[9]H. Schmidt, G. Jura, and J. H. Hildebrand, J. Phys. Chem. 63, 297 (1959).

[10]M. Fixman, J. Chem. Phys. 36, 1961 (1962).

[11]P. A. Egelstaff and T. W. Ring, in *Physics of Simple Liquids*, edited by H. N. V. Temperley (North-Holland, Amsterdam, 1968), Chap. 7.

[12]V. P. Skripov and V. M. Kostin, Russ. J. Phys. Chem. 34, 718 (1960).

[13]Yu. P. Blagoi and V. G. Gusak, Zh. Eksperim. i Teor. Fiz. 56, 592 (1969) [Sov. Phys. JETP 29, 326 (1969)].

[14]J. P. Brouwer, A. M. Vossepoel, C. J. N. Van Den Meijdenberg, and J. J. M. Beenakker, Physica 50, 125 (1970).

[15]T. Alvesalo, P. Berglund, S. Islander, G. R. Pickett, and W. Zimmermann, Jr., Phys. Rev. Letters 22, 1281 (1969).

[16]Landolt-Börnstein, *Zahlenwerte und Funktionen* (Springer, Berlin, 1967), 6th ed., Vol. IV, p. 916; and Vol. II, p. 482.

[17]P. Heller, Rept. Progr. Phys. 30, 731 (1967).

PHYSICAL REVIEW B VOLUME 6, NUMBER 2 15 JULY 1972

Electron Momentum Distribution in Vanadium*

T. Paakkari, S. Manninen, O. Inkinen, and E. Liukkonen
Department of Physics, University of Helsinki, SF-00170 Helsinki 17, Finland
(Received 20 December 1971)

The Compton profile of polycrystalline vanadium has been measured using 59.54-keV γ rays from an ^{241}Am source. In the regions of medium and high electron momentum, the observed profile coincides with that calculated from Hartree-Fock free-atom wave functions for the outer-electron configuration $3d^4 4s$. At small momentum values the experimental results deviate significantly from those predicted by Hartree-Fock theory.

I. INTRODUCTION

The importance of momentum distributions has long been recognized in x-ray Compton scattering from electronic systems.[1] Only very recently, however, have the measurements been productive. A wide range of systems has been studied at Mo$K\alpha$ or Ag$K\alpha$, including inert gases,[2] diatomic[2,3] and polyatomic[4-7] molecules, and light crystalline elements and compounds.[8] All these experiments have yielded decisive information about the electron momentum distributions.

Another possibility for studying the electron momentum density is the Compton scattering of γ rays. A suitable radioactive source is, for example, ^{241}Am, which emits 59.54-keV photons. The use of ^{241}Am γ rays and a solid-state detector in conjunction with a multichannel analyzer instead of Mo$K\alpha_1\alpha_2$ (17 keV) or Ag$K\alpha_1\alpha_2$ (22 keV) x rays and a crystal spectrometer offers some advantages.

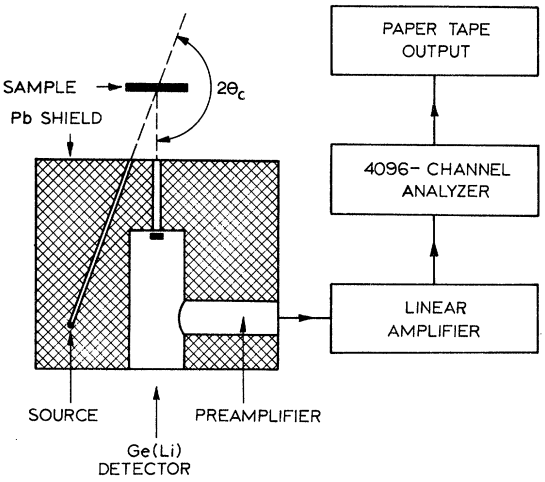

FIG. 1. Schematic drawing of the experimental arrangement.

(i) The relative contribution of the inelastic scattering increases and the electron binding effects decrease with increasing energy of the incident photon; this makes it possible to extend the Compton measurements to relatively heavy materials. (ii) The uncertainties in the data-reduction procedure which arise from the doublet nature of the incident beam and the wavelength-dependent corrections due to the analyzing crystal are eliminated. (iii) The measuring time needed to attain the desired statistical accuracy is radically reduced. (iv) The background scattering is very much smaller due to the absence of bremsstrahlung. A disadvantage is that the energy resolution of the solid-state detectors at 60 keV is lower than that of a LiF analyzing crystal employed at Mo$K\alpha$ and Ag$K\alpha$. However, the important value in the Compton-profile measurements is the ratio of the width of the Compton profile to that of the energy-resolution function. When a solid-state detector is used, this ratio increases with increasing energy of the incident photon, but decreases in the case of a crystal analyzer.

It has been realized for some time that the Compton-profile measurement constitutes a very powerful probe for transition metals. The first measurement, done with sufficient accuracy to determine the momentum density, was that of Weiss[9] on titanium at Mo$K\alpha$. The valence-electron momentum density evidenced significant 4*s* character, and in the high-momentum region a marked discrepancy was found between the experimental Compton profile and that calculated from Hartree-Fock (HF) free-atom wave functions. In contrast with Weiss's results, the Compton profile of iron, measured by Felsteiner *et al.*[10] at 59.54 keV, was in good agreement with that computed from HF wave functions with seven 3*d* electrons. Also the Compton profile of scandium, measured by Manninen[11] at Mo$K\alpha$, agreed with HF profile in the high-momentum region.

The present work is aimed at securing information about the electron momentum distribution in vanadium by measurement of the Compton profile with γ rays.

II. EXPERIMENTAL PROCEDURE

The experimental arrangement is shown schematically in Fig. 1. γ rays from a 45-m Ci ^{241}Am point source having an active diameter of 3 mm were used to irradiate the sample of polycrystalline vanadium, which was prepared in a mold under uniaxial pressure. The sample diameter was 2 cm, thickness was 2.7 mm, and the density in relation to bulk density was 0.57. The incident beam was collimated by a cylindrical lead collimator of length 14 cm and diameter 3 mm. After the γ rays were scattered by the sample through a mean angle of $2\theta_c = 160°$, they passed through a second lead collimator of length 5 cm and diameter 5 mm. This collimator was set in front of a Ge(Li) detector (active diameter 10 mm, sensitive depth 5 mm, Be window 0.13 mm) to minimize the air scattering and to reduce the number of photons which are able to escape from the detector. The detector was followed by a preamplifier, a linear amplifier, and a 4096-channel analyzer, which was operated in a 4×1024 mode.

The raw experimental data (counts accumulated during a period of 80 h) are indicated in Fig. 2. The spectrum of the scattered γ rays consists of a Compton line and an elastic component both superimposed on a smooth background. The Compton peak-to-background ratio is approximately 25 to 1.

A separate experiment was made to determine the fraction of air scattering in the scattered beam. At first the air scattering was measured when the sample was removed. From the data obtained, the contribution of air scattering to the scattered intensity when the sample is at the position shown in Fig. 1, could be evaluated by taking account of the effect of sample absorption. The air-scattering correction was found to be about 0.5% for the total scattered intensity and less than 1% at the Compton peak.

The first step in data reduction was to subtract the background from the accumulated counts corrected for air scattering. A correction was then applied to the data to account for the energy dependence of the absorption of γ rays in the sample. The corrected values were obtained by multiplying the observed ones by the factor

$$\frac{\mu_0+\mu\sin\alpha/\sin\beta}{1-\exp[-d(\mu_0\operatorname{cosec}\alpha+\mu\operatorname{cosec}\beta)]},$$

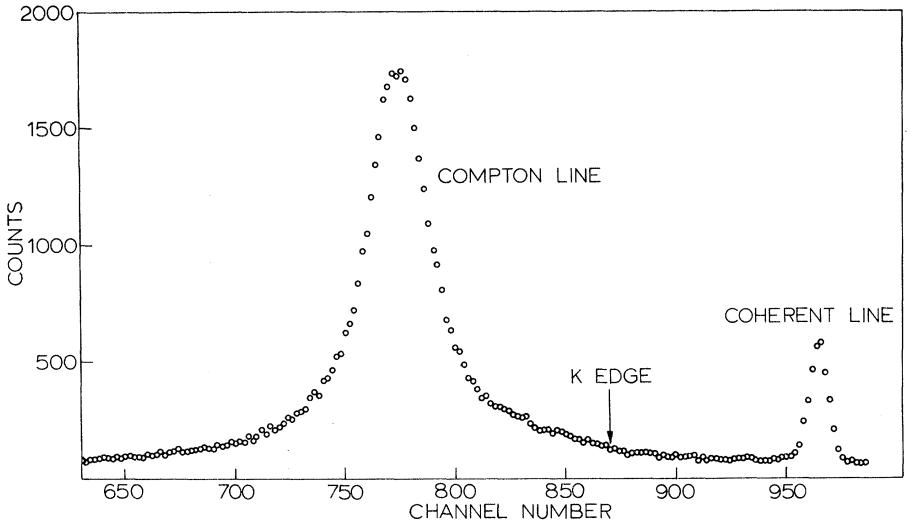

FIG. 2. Raw experimental data for vanadium. Accumulated counts for every second channel are plotted versus the channel number. The channel width corresponds to a γ-ray energy of 57.10 eV.

where μ_0 and μ are the linear absorption coefficients of the sample, of thickness d, for the incident and scattered γ rays, and α and β are the angles between the sample surface and the incident and scattered beams. The absorption correction was taken to be zero at the coherent peak, and was about 20% in the low-energy tail of the Compton profile. The final correction came from the inclusion of the Breit-Dirac factor and the relativistic effects. The so-called relativistic Breit-Dirac factor $(E/E_0)^3$ (E_0 and E are the energies of the incident and scattered photons, respectively), which is commonly used at x-ray energies (cf. Ref. 8, p. 461), is not accurate enough in the present case. Klein and Nishina[12] have shown that in the rest system of the initial free electron the relativistic differential cross section is given by

$$\frac{d\sigma}{d\Omega} \propto \left(\frac{E}{E_0}\right)^3 + \frac{E}{E_0}\left(1 - \frac{E}{E_0}\sin^2 2\theta_c\right).$$

Accordingly, the measured Compton profile $J(E)$ was divided point by point by $d\sigma/d\Omega$. The Compton profile arrived at after corrections is shown in Fig. 3.

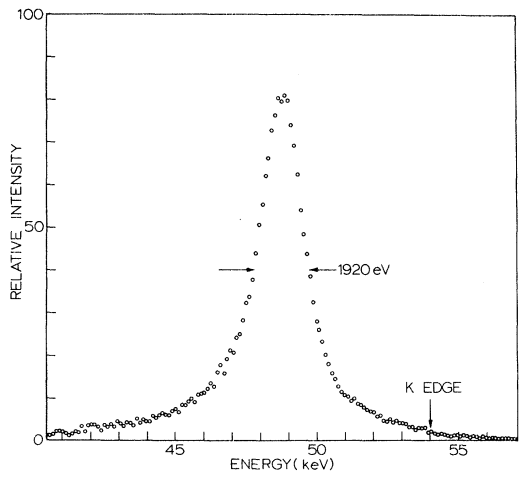

FIG. 3. Corrected Compton profile of vanadium. The background and the contribution of air scattering have been subtracted, and the corrections for sample absorption, the Breit–Dirac factor, and the relativistic effects made. The asymmetry of the profile is mainly attributable to the low-energy tail of detector's resolution function (see Fig. 4) and the contribution of the 1s electrons, which appears in the energy region below the K edge.

The sources of line broadening arose from the finite energy resolution of the Ge(Li) detector, and from the finite range of the scattering angle. The energy-resolution function of the detector was measured at 59.54 keV by replacing the scattering sample by a low-intensity ^{241}Am source. The resulting curve is shown in Fig. 4, from which a value of 580 eV is obtained for the full width at half-maximum (FWHM). From a study of the energy dependence of resolution, a FWHM of 560 eV was found at the Compton peak (about 48.5 keV). To correct for the 20-eV difference observed, the measured Compton profile was convolved with a Gaussian function of half-width 150 eV. The variation of the energy resolution along the Compton line was neglected. Further, the corrections due to the escape-peak-to-photopeak ratio and the efficiency of the detector could be ignored, because the escape-peak-to-photopeak ratio is less than 1% for a well-collimated Ge(Li) detector, and the efficiency is constant in the energy region 45–60 keV.[13,14]

A range $d\theta_c$ in the scattering angle produces an uncertainty dE_{Cpt} in the Compton-energy shift, which is given by

$$dE_{\mathrm{Cpt}} \simeq -2E^2 \sin 2\theta_c d\theta_c / mc^2.$$

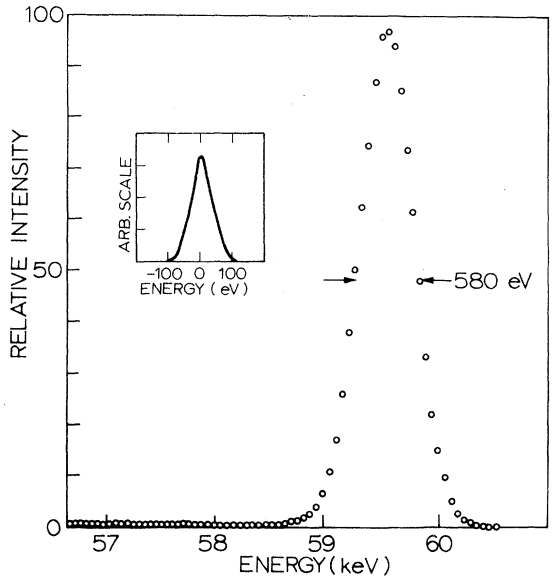

FIG. 4. Energy-resolution function of the Ge (Li) detector at 59.54 keV and that defined by the geometrical factors (inset). The low-energy tail of the photopeak is mainly effected by the γ rays which are Compton scattered within the detector, deposited some of their energy, and then escaped the detector.

The distribution of scattering angles produced by the geometrical factors, such as horizontal divergence and the shape of collimators, was calculated using a computer program. The resultant resolution function is shown in the inset of Fig. 4. The

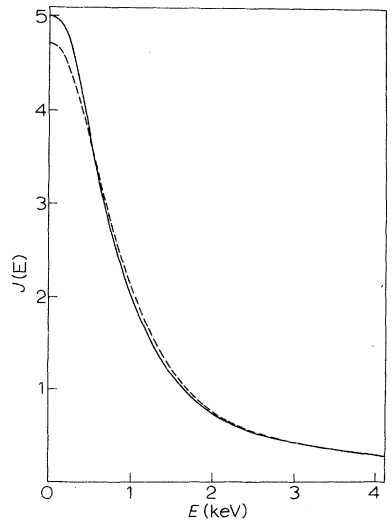

FIG. 5. Effects of finite instrumental resolution on the measured Compton profile. The dashed curve is the high-energy side of the profile from Fig. 3, and the full curve is the true Compton profile obtained by a trial-and-error deconvolution program.

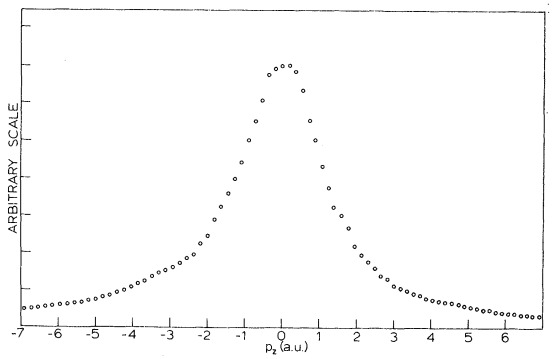

FIG. 6. Un-normalized Compton profile after the removal of the effects of instrumental resolution and the conversion to an electron- momentum scale.

FWHM for the slightly asymmetrical curve is about 100 eV, which corresponds to a range $\pm 2^\circ$ in the scattering angle.

The effects of finite instrumental resolution on the measured Compton profile are illustrated in Fig. 5. The true Compton profile was obtained by an iterative procedure in which successive trial profiles were convolved with the known instrumental-resolution function until agreement with the measured profile was found. The effect of resolution corrections on the FWHM of the profile was found to be about 9%. Finally, the true profile was converted from a γ-ray energy to an electron momentum scale through the relation

$$p_z = \left(\frac{\Delta E}{E}\,\frac{mc}{2\sin\theta_c} - \frac{E_0}{c}\sin\theta_c\right) \times \left[1 + \frac{\Delta E}{E} + \left(\frac{\Delta E}{E}\right)^2 (2\sin\theta_c)^{-2}\right]^{-1/2},$$

where p_z is the component of electron's initial momentum along the scattering vector, and $\Delta E = E_0 - E$. The resulting curve $J(p_z)$ is indicated in Fig. 6.

The low-energy side of the Compton profile (Fig. 3) is more affected by uncertainties attributable to the long low-energy tail of detector's energy-resolution function (Fig. 4), the separation of background, and the absorption correction than the high-energy side. Thus, in spite of the uncertainty caused by the 1s edge, the high-energy side is obtained more accurately in the deconvolution. Accordingly, the high-energy half of the experimental Compton profile $J(p_z)$ will be used for comparison with theoretical values. The area under that curve was normalized to one-half the total number of electrons per atom minus the impulse-approximation contributions of the 1s, 2s, and 2p electrons above $p_z \simeq 8.5$ a.u., which corresponds to the K binding energy.

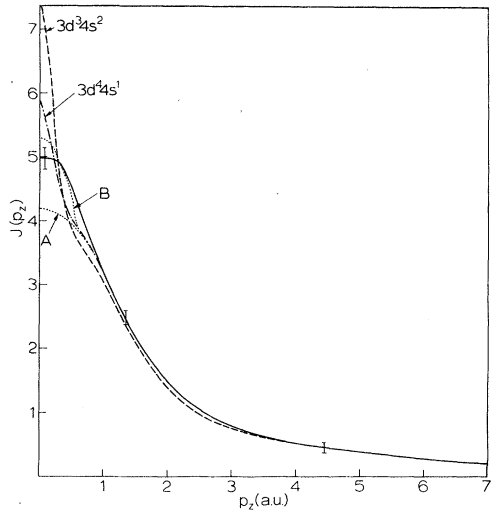

FIG. 7. Experimental and calculated Compton profiles of vanadium. The full curve refers to experiment. The experimental error indicated for some points includes the contribution from counting statistics and the uncertainties due to background, air scattering, and absorption corrections; the total error at $p_z=0$ amounts to about 4%. The curves marked $3d^3\,4s^2$ and $3d^4\,4s$ are calculated from Hartree-Fock free-atom wave functions including the $1s^2\,2s^2\,2p^6\,3s^2\,3p^6$ core. Curve A represents the Hartree-Fock profile for the electrons $1s^2\,2s^2\,p^6\,3s^2\,3p^6\,3d^4$, and curve B is arrived at as a superposition of curve A and the profile calculated from free-electron theory for one free electron per atom.

III. RESULTS AND DISCUSSION

The final normalized Compton profile $J(p_z)$ is shown in Fig. 7 together with the profiles calculated from Clementi's[15] HF free-atom wave functions for the outer-electron configurations $3d^3\,4s^2$ and $3d^4\,4s$. Included also is the HF profile calculated for the electrons $1s^2\,2s^2\,2p^6\,3s^2\,3p^6\,3d^4$ (curve A), and the profile (curve B) obtained as a superposition of curve A and the profile calculated from free-electron theory for one free electron per atom. In the free-electron theory,

$$J(p_z)=3n(p_F^2-p_z^2)/4p_F^3\ ,$$

where n is the number of free electrons per atom, and $p_F=\frac{1}{2}h(3\rho/\pi)^{1/3}$ is the Fermi momentum, with ρ representing the density of free electrons.

It can be seen from Fig. 7 that in the region $p_z\geq 1$ a.u., the experimental Compton profile coincides with HF profile calculated for the outer-electron configuration $3d^4\,4s$. This indicates that the inner-electron momentum distribution is not changed upon going from the free atom to the metallic state, and that the conduction band of vanadium is occupied by one 4s electron. These observations are in agreement with the results of Felsteiner *et al.*[10] on iron. Also in the case of scandium,[11] the inner-electron states are well described by HF wave functions, in contrast with the results of Weiss[9] on titanium. At small momentum values, where the calculated profiles are most sensitive to the outer-electron wave functions, the experimental results of vanadium deviate significantly from those predicted by HF theory. It is interesting to note that a marked improvement over the agreement obtained with HF wave functions is found if the Compton profile of 4s electron is calculated from free-electron theory. The discontinuity in the slope of the calculated profile B at $p_z\simeq 0.7$ a.u., which is associated with the Fermi surface, does not appear in the experimental profile. As demonstrated by Fig. 8, in which the low-momentum part of the experimental profile is compared with the curve obtained as a convolution of profile B and the instrumental-resolution function, this discrepancy is solely attributable to the limited experimental resolution.

By way of summary, it can reasonably be concluded that the outer-electron configuration in vanadium is $3d^4\,4s$. This is in agreement with the augmented-plane-wave calculations of Snow and Waber[16] on vanadium, which favor an occupancy nearer to $3d^4\,4s$ than $3d^3\,4s^2$. Although the experimental Compton profile is quite close to the $3d^4\,4s$ profile (4s electron free), it appears that a solid-state calculation will be necessary to further improve the agreement with the Compton-profile measurement.

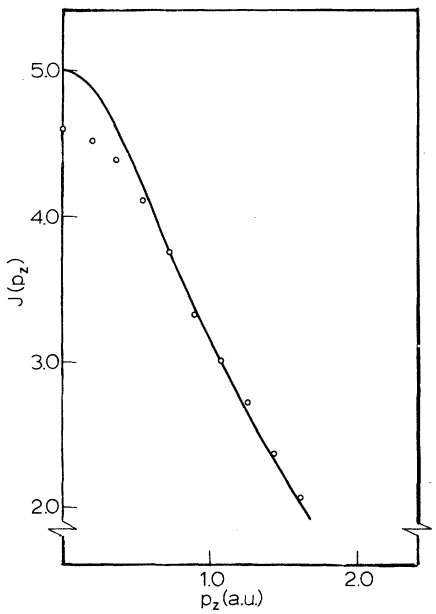

FIG. 8. Low-momentum part of the experimental Compton profile (points), and the curve obtained as a convolution of the calculated profile B in Fig. 7 and the instrumental-resolution function.

ACKNOWLEDGMENTS

The authors wish to thank Miss Mervi Hyvönen, M. Sc., and Mrs. Riitta Vahtola for their help with the computational work.

*Work supported in part by the National Research Council for Sciences, Finland.

[1]J. W. M. DuMond, Rev. Mod. Phys. 5, 1 (1933).
[2]P. Eisenberger, Phys. Rev. A 2, 1678 (1970).
[3]M. Cooper and B. Williams, Phil. Mag. 22, 543 (1970).
[4]M. Cooper, M. Roux, M. Cornille, and B. Tsapline, Phil. Mag. 18, 309 (1968).
[5]R. J. Weiss, J. Chem. Phys. 52, 2237 (1970).
[6]O. Inkinen, V. Halonen, and S. Manninen, Chem. Phys. Letters 9, 639 (1971).
[7]P. Eisenberger and W. C. Marra, Phys. Rev. Letters 27, 1413 (1971).
[8]For review, see M. Cooper, Advan. Phys. 20, 453 (1971).
[9]R. J. Weiss, Phys. Rev. Letters 24, 883 (1970).
[10]J. Felsteiner, R. Fox, and S. Kahane, Solid State Commun. 9, 457 (1971).
[11]S. Manninen, J. Phys. F 1, L60 (1971).
[12]O. Klein and Y. Nishina, Z. Physik 52, 853 (1929).
[13]V. W. Slivinsky and P. J. Ebert, Nucl. Instr. Methods 71, 346 (1969).
[14]J. M. Palms, P. Venugopala Rao, and R. E. Wood, Nucl. Instr. Methods 64, 310 (1968).
[15]E. Clementi, IBM J. Res. Develop. Suppl. 9, 2 (1965).
[16]E. C. Snow and J. T. Waber, Acta Met. 17, 623 (1969).

PHYSICAL REVIEW B VOLUME 6, NUMBER 2 15 JULY 1972

Lattice Thermal Conductivity of a Neutron-Irradiated Copper-Aluminum Alloy*

A. J. Friedman,† T. K. Chu, P. G. Klemens, and C. A. Reynolds‡
Department of Physics and Institute of Materials Science, University of Connecticut, Storrs, Connecticut 06268
(Received 24 January 1972)

Low-temperature thermal-conductivity results are presented on two Cu+9-at.%-Al polycrystals which show that fast-neutron irradiation has two effects on a coldworked sample of this alloy. In the well-annealed specimen, irradiation produced defects which scatter long-wavelength phonons, giving a well-defined T^{-2} contribution to the lattice thermal resistivity. Observations by other authors using electron microscopy suggest that the defects are planar-vacancy-generated dislocation loops 75–100 Å in diameter. The loop density is calculated from the thermal resistivity and is found to be in reasonable agreement with the electron-microscopy results. In the second sample, deformed in tension at room temperature and then annealed at 573 °K prior to irradiation, the same irradiation treatment produced a contribution to the lattice resistivity which was similar in temperature dependence but larger, by a factor of 3, than that produced in the well-annealed specimen. A model for this effect is suggested, based on two distinct contributions to the radiation-produced thermal resistivity: (i) dislocation loops of similar size and concentration as in the well-annealed sample; (ii) reformation of solute atmospheres around dislocations. These atmospheres had been thermally dispersed by annealing; their reformation is due to enhanced solute diffusion resulting from a large vacancy concentration produced by irradiation. The work of Mitchell *et al.* has shown that solute atmospheres in Cu+10 at.% Al enhances phonon scattering by dislocations.

I. INTRODUCTION

Recent theoretical and experimental work has shown that the study of phonon scattering in alloys, using low-temperature thermal-conductivity measurements, can yield information about the equilibrium arrangement of solute atoms in the strain fields of dislocations, i.e., impurity atmospheres, and about the rate at which this equilibrium is attained. The theory of the modification of dislocation thermal resistivity at low temperatures by impurity atmospheres (Klemens,[1,2] Ackerman and Klemens[3]) was substantiated by Mitchell *et al.*[4] in a study of the annealing characteristics of the dislocation thermal resistivity in Cu+10-at.%-Al polycrystals. These experiments also indicated enhanced diffusion of the solute atoms during deformation, causing rapid formation of the impurity atmospheres. It was suggested that vacancies produced during plastic deformation could account for this enhancement.

In this paper we report on a series of low-temperature thermal-conductivity measurements which attempt to determine if fast-neutron irradiation can also produce the enhanced diffusion necessary for impurity-atmosphere formation. Two Cu+9-at.%-Al polycrystals were studied. One was irradiated in the well-annealed condition to determine if any extended damage was produced which would give rise to phonon scattering in the temperature range